9th International Conference on Fracture Mechanics of Concrete and Concrete Structures
FraMCoS-9
V. Saouma, J. Bolander, and E. Landis (Eds)
DOI 10.21012/FC9.032

PLASTIC SHRINKAGE OF INERT AND CEMENT-BASED MATERIALS: CHARACTERIZATION AND COMPARISON

D. LUO[†], F. BEGAUD[†], A. DELAPLACE[*†] AND M. VANDAMME[‡]

[†]LafargeHolcim Research Center
Saint Quentin Fallavier, France
e-mail: arnaud.delaplace@lafargeholcim.com

[‡]Ecole des Ponts ParisTech - Laboratoire Navier
Champs-sur-Marne, France
e-mail: matthieu.vandamme@enpc.fr

Key words: Plastic shrinkage, cracking, early-age behavior

Abstract. The plastic behavior of inert and cement-based materials is analyzed in this study. We show that a Cam-Clay-based model is relevant to describe the consolidation regime of the material during the plastic regime. For inert materials, the model is successfully used to evaluate the capillary pressure corresponding to the plastic cracking. To assess the cracking risk of the material, the volumetric deformation, the mechanical behavior in the plastic regime and the air entry pressure have to be characterized.

1 INTRODUCTION

Understanding of plastic regime behavior is of main interest for cement-based materials, as cracking may occur in this early-age stage. Although all mechanisms are not yet described at microscale, the phenomena at mesoscale are quite well understood: (i) water bleeding occurs simultaneously to material segregation, (ii) when bleeding water disappears due to drying, menisci appear at material surface and capillary pressure increases into the material, (iii) leading eventually to cracking [1–3].

This study focuses on finding a simple approach to compare the risk of plastic cracking for different materials. In a first part, five types of inert fillers, known to have different plastic cracking risks, have been considered. Four laboratory tests have been performed: early-age shrinkage, air entry pressure, œdometer test, crack-band tests. The experimental results validate the use of a simple Cam-Clay-based model to describe the plastic regime. We show that the identified model parameters can be correlated to the risk of plastic cracking for these materials.

In a second part, two cement-based materials are considered. The main difference with the inert materials is that material properties evolve with material hydration, hence making it more complicated to perform the experiments. For these materials, we succeed into capturing the evolution of the material properties over time, especially those measured with the oedometer test. Finally, using the relationship found for inert materials, we propose a strategy to classify the materials according to their risk of plastic cracking.

2 CHARACTERIZATION OF PLASTIC BEHAVIOR

Early-age behavior of cementitious materials (before setting) is close to the behavior of a soil and the material can be seen as a saturated granular media. The driving force at early age

is the development of a capillary pressure due to drying, which manifests itself when the evaporation rate exceeds the material bleeding [7].

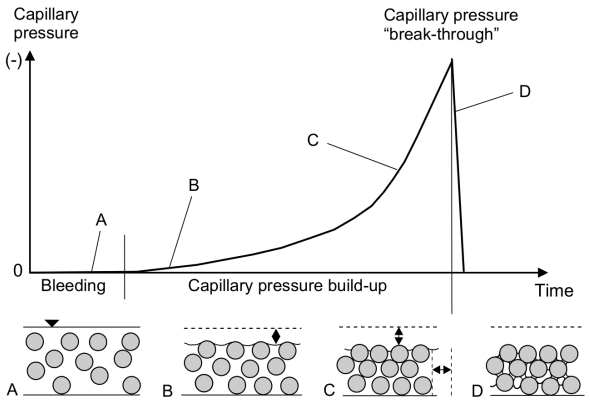

Figure 1: Development of capillary pressure [7].

To describe the behavior of the material before cracking, we refer to the work of Radocea [5], who introduced a plastic modulus H linking the vertical strain ε_{zz} and the settlement u as $H = -\partial u/\partial \varepsilon_{zz}$. This evolution is similar to the behavior of a soil for which the strain ε increases with the logarithm of the effective stress. The well-known Cam-Clay model is able to describe such behavior (figure 2) [6]: a first elastic regime is characterized by a slope $\kappa/(1+e_0)$, a second plastic regime is characterized by a slope $\lambda/(1+e_0)$, where e_0 is the void ratio in the state of reference.

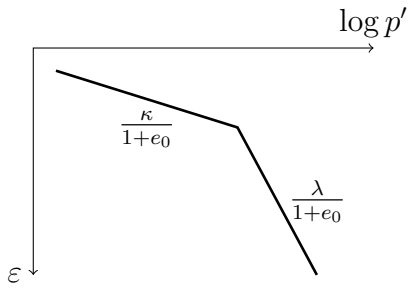

Figure 2: Cam Clay model

We propose a modified version of the Cam-Clay model allowing a zero-deformation if there is no capillary pressure (state A in figure 1). The deformation reads:

$$\varepsilon = \frac{\lambda}{1+e_0} \log\left(\frac{p'}{P_0}+1\right) \qquad (1)$$

where p' is the effective volumetric stress, defined as the total stress minus the pore water pressure, and P_0 is a characteristic pressure.

Following the plastic regime, cracking can only occur if water evaporation rate exceeds bleeding water, leading to formation of meniscus on top surface. Capillary pressure increases, and when the curvature of meniscus is to important, air starts penetrating large capillary pores. The capillary pressure at which such event occurs is called the air entry pressure. Slowik *et al* [7] assume that it corresponds also to cracking, although we will show that the full picture may be more complex.

To assess the plastic risk of the material, one needs the following properties:

- the Cam-Clay parameters,
- the air entry pressure,
- the evolution of the capillary pressure,
- the volumetric variation,
- a cracking state.

Experiments used in this study are:

- Œdometer test: a one-dimensional consolidation is considered, following the ASTM Standard Test Method D2435.
- Air entry pressure: the method proposed by [8] is used (figure 3): the bottom of the cell is connected to compressed air. The air pressure is increased until air penetrates into the sample. The test is stopped when bubbles are visible on the top of the cell.

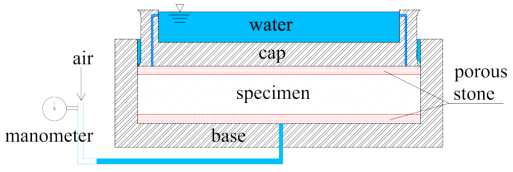

Figure 3: Measurement of air entry pressure [4].

- Free-shrinkage bench: the bench allows to record the evolution of the vertical, longitudinal deformations (and hence the volumetric deformation) as well as the capillary pressure (figure 4).

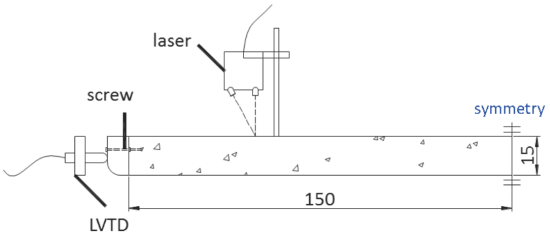

Figure 4: Sketch of the free-shrinkage bench. The capillary pressure is measured using a capillary sensor located at the mid-height of the sample.Dimension unit is mm.

- Cracking test: we use a mold that makes it possible to cast a set of parallel bands (or mini-slabs) of materials, as shown in figure 5, located in a temperature and humidity-controlled room ($T = 20°C$, 65% relative humidity). Once the mini-slabs are cast, we let them dry. A camera is used to obtain the time of occurrence of the first and last cracks.

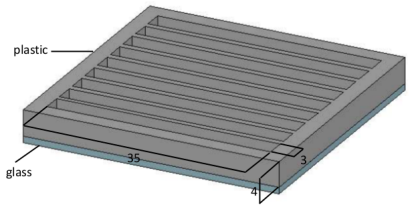

Figure 5: Sketch of the bands to observe cracking state of material. Dimension unit is cm.

3 RESULTS ON INERT MATERIALS

We present first results obtained on inert materials. Contrary to cement-based materials, the grain size distribution of such materials is assumed to be constant with time, allowing an easiest analysis of results. Five different calcium carbonate powders are studied, denoted from P1 to P5, with grain size distribution represented on figure 6. These powders are used for screed mix-designs. They are known to exhibit different sensitivities regarding the plastic cracking risk. Table 1 gives a rough classification of the powders based on field observations, assuming an equivalent mix design and same external drying conditions.

Table 1: Plastic cracking risk of inert powders

Powder	Risk of cracking
P1, P2	high
P3	medium
P4, P5	low

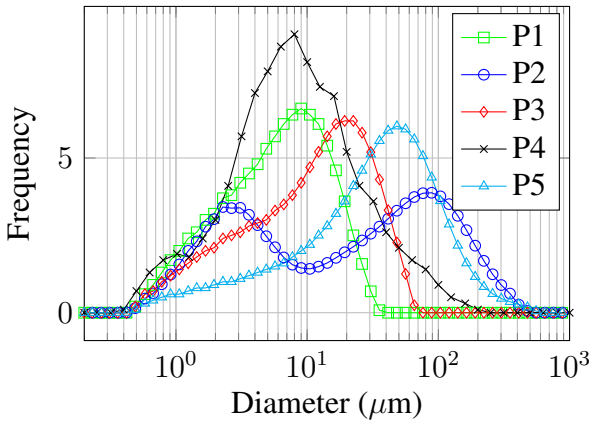

Figure 6: Grain size distributions of the five studied powders.

3.1 Cam-Clay parameters

The Cam-Clay parameters are obtained using the œdometer test on cylinder (diameter: 7 cm, thickness: 2 cm), with 11 loading steps ranging between 0.1 and 4 kN. An output is shown on figure 7 for inert material P2.

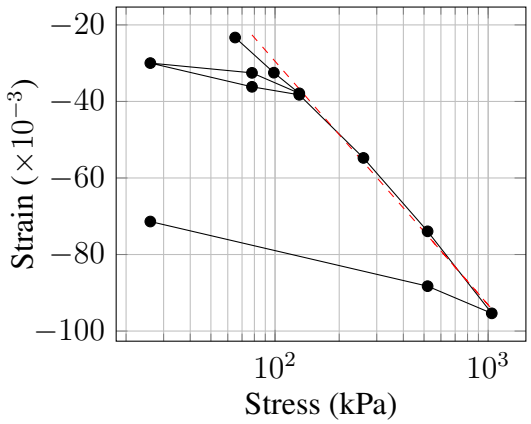

Figure 7: Result of œdometer test for powder P2. The red dashed line is the best fitted slope for the plastic regime, which provides the parameter $\lambda/(1+e_0)$.

The elastic slope is obtained on the unloading part of the curve, the plastic slope is measured on the asymptotic behavior of the evolution. To obtain the Cam-Clay parameters κ and λ, one needs to compute the initial void ratio e_0, *i.e.* the value of the void ratio when bleeding water has evaporated. It is computed as:

$$e_0 = \frac{V_{w0} - \Delta V_b}{V_0 - V_{w0}} \tag{2}$$

where V_{w0} is the initial water volume, V_0 is the initial volume of the sample, ΔV_b is the bleeding quantity.

The results obtained for the inert materials are given in table 2, together with the volume variation at the end of the free-shrinkage bench experiment.

Table 2: Cam-Clay and free-shinkage bench properties of inert powders

Material	P1	P2	P3	P4	P5
e_0	1.05	0.63	0.81	0.69	0.61
$\frac{\kappa}{1+e_0}(\times 10^{-3})$	6.9	6.2	2.4	-	2.2
$\frac{\lambda}{1+e_0}(\times 10^{-2})$	2.7	2.6	1.9	1.5	1.5
Vol. variation	0.17	0.22	0.19	0.13	0.11

3.2 Plastic cracking and air entry pressure

The cracking state is characterized by the time of appearance of first crack and of the last one (stabilized state). We also consider the cracking pattern (crack spacing) but this consideration is not used in the present study. The air entry pressure and the cracking time are given in table 3 for powders P1, P3 and P5.

Table 3: Air entry pressure and time at occurrence of first crack for inert powders

Material	P1	P3	P5
P_{AE} (kPa)	270	150	70
Cracking time (mn)	2490	2865	2122

3.3 Validation of the model

We propose next to validate the consolidation behavior described by the Cam-Clay model on the real plastic regime of the inert materials. For each material, the evolution of the longitudinal, vertical variations, the capillary pressure, the mass loss, the cracking state are recorded. An example of evolution is presented on figure 8. Note that the drop of the capillary pressure is due to the limit of the capillary sensor, not to the material behavior.

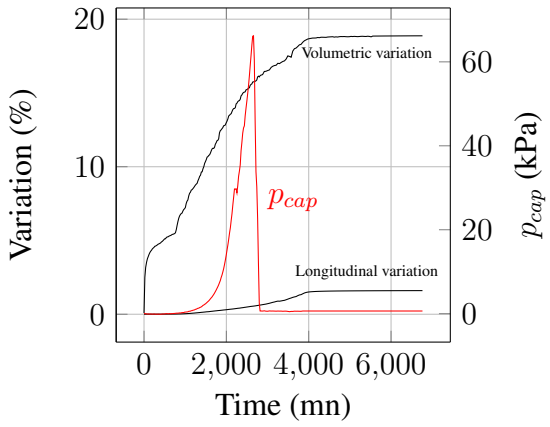

Figure 8: Evolution of deformation and capillary pressure for P3 inert material.

From these evolutions, we can plot the evolution of the deformation versus the logarithm of the capillary pressure (figure 9). The response of the Cam-Clay model using the parameters obtained from the œdometer test is plotted on the same graph. A nice agreement is obtained

between the two responses for the plastic linear part, validating the consolidation behavior of the material in the plastic regime.

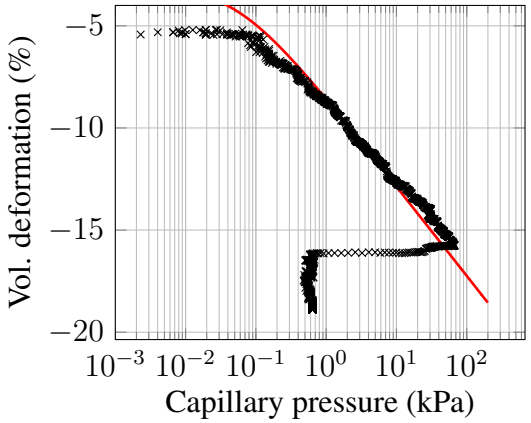

Figure 9: Volumetric deformation vs. capillary pressure for P3 inert material. The red curve is the Cam-Clay model response using parameters of table 2.

Finally, the capillary pressure corresponding to cracking time is estimated using the identified Cam-Clay parameters, as the used capillary sensors are not able to reach this pressure. Table 4 give the comparison between the measured air-entry pressure and the estimated capillary pressure at cracking. Results show that, when cracking occurred, the capillary pressure was smaller than (for material P1) or close to (for material P3 and P5) the air entry pressure.

Table 4: Air entry pressure and estimated capillary pressure when cracking occurred (kPa)

Material	P1	P3	P5
P_{AE}	270	150	70
Cracking capillary pressure	165	153	87

3.4 Conclusion on inert materials

Plastic regimes of inert material can be described accurately by a Cam-Clay model. In the consolidation regime, a linear relationship is obtained between the material deformation and the logarithm of the capillary pressure. When cracking occurred, the capillary pressure was smaller than or close to the air entry pressure. Therefore, one can interpret the air entry pressure as the magnitude of the capillary pressure that is the most harmful for the material, in terms of risk of cracking. This can be well understood with poromechanics: in first order, the mechanical stress exerted by the pore water on the porous solid can be approximated by the product of the capillary pressure with the liquid saturation, which decreases once the capillary pressure becomes greater than the air entry pressure.

From these results, the following phenomenological correlations are observed: plastic cracking risk increases with the air entry pressure, the Cam-Clay plastic slope, the final volume variation (except for powder P1 in this study, see table 2). Also, although it is not a generic rule, an inert material with finer grains is more prone to cracking, as a consequence of its greater air entry pressure.

Finally, from the rate of evaporation and the Cam-Clay parameters of the material, one can estimate the time at which the capillary pressure will reach the air entry pressure.

4 RESULTS ON CEMENT-BASED MATERIALS

The same approach has been applied to two cement-based materials: a cement paste and a mortar. The analysis is much more complicated as the material microstructure evolves with time. Then, the œdometer test has to be done at different times. Figure 10 shows the evolution of the Cam-Clay parameters for both cement-based materials before setting time, and also after setting time for cement paste.

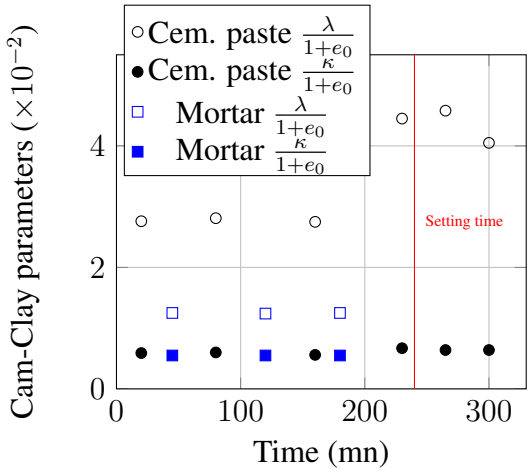

Figure 10: Evolution of Cam-Clay parameters for cement-based materials. The vertical line represents the setting time.

Based on this experiment, one can observe that:

- The elastic slope $\frac{\kappa}{1+e_0}$ is constant over time (and is very similar for the two tested materials)
- The plastic slope $\frac{\lambda}{1+e_0}$ is quasi-constant before the setting time, and increases to a second constant value after the setting time.

Then, we make the assumption that before the setting time, the consolidation regime observed for inert materials is also relevant for cement-based materials, even if the microstructure evolves during this period. After the setting time, the consolidation theory is no more relevant as the material behavior is close to an elastic behavior of solid.

Figures 11 and 12 give the evolution of the variation, the capillary pressure for both cement-based materials. As for the inert materials, we observe that the capillary pressure starts to increase with the longitudinal deformation, *i.e.* when no more bleeding water is available for drying.

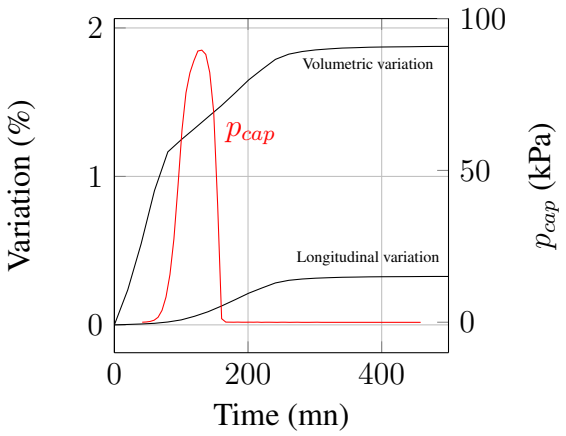

Figure 11: Evolution of deformation and capillary pressure for cement paste.

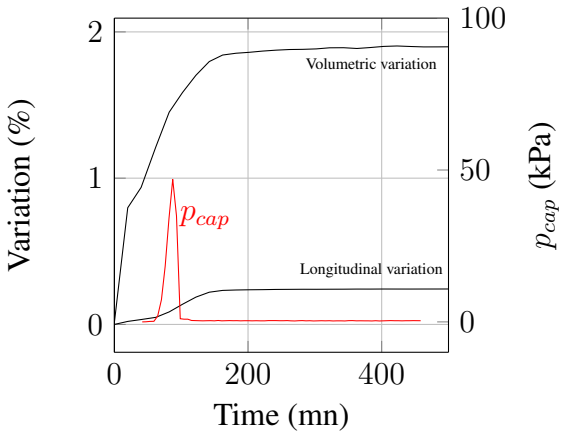

Figure 12: Evolution of deformation and capillary pressure for mortar.

From these curves, we can plot the evolution of the volumetric deformation vs. the capillary pressure, and make the comparison with the Cam-Clay model with the parameters obtained in figure 10.

The agreement between the model and the experimental response is very good for the cement paste. The transition between the plastic regime and the solid response is clearly visible, and corresponds approximately to the setting time. Although the result for the mortar is a bit disappointing and needs further investigation, we can claim that the Cam-Clay model is relevant to describe the plastic regime of a cement-based material. In a first approximation, the model parameters λ and κ can be as-

sumed to be constant before the setting time, even if the material microstructure evolves. Parameters change after the setting time as the material becomes solid.

The next step will be to evaluate the capillary pressure corresponding to the cracking time. This work is under progress.

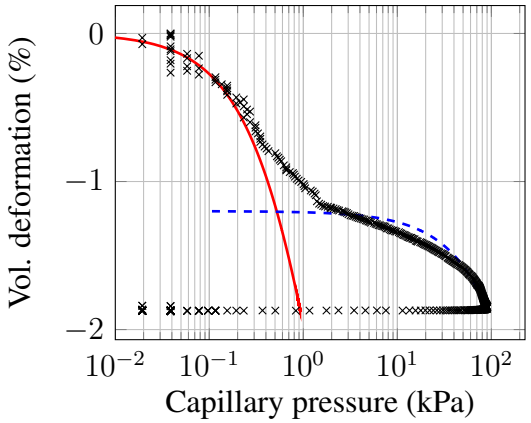

Figure 13: Volumetric deformation vs. capillary pressure for cement paste. The red curve is the Cam-Clay model response using parameters obtained in figure 10 before setting time, the blue dashed curve is a linear evolution corresponding to the behavior of an elastic solid material.

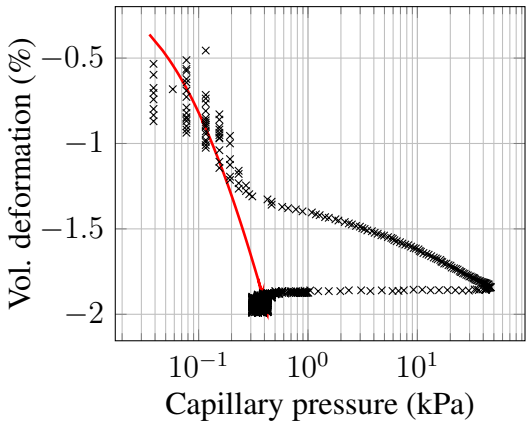

Figure 14: Volumetric deformation vs. capillary pressure for mortar. The red curve is the Cam-Clay model response using parameters obtained in figure 10.

5 CONCLUSIONS

Plastic regimes of inert and cement-based materials have been studied using a Cam-Clay model. Good agreement between the model and the experimental results has been found, especially for cement-based materials for which the assumption of constant values of model parameters can be done before setting time.

For inert materials, the model has been applied with success to evaluate the capillary pressure corresponding to the initiation of cracking. We could infer that cracking always started at a capillary pressure lower than or close to the air entry pressure. Such observation suggests that one can interpret the air entry pressure as the magnitude of the capillary pressure that is the most harmful for the material, in terms of risk of cracking.

However, the volumetric deformation, the plastic slope of the Cam-Clay model, and the air entry pressure have to be considered globally to determine the risk of cracking: anyone of those parameters is not sufficient to comprehend the full complexity of the phenomenon.

REFERENCES

[1] William, L. 1957. Plastic Shrinkage, *Journal of ACI*, **28**:797–802.

[2] Cohen, M.D., Olek, J. and Dolch, W.L. 1990. Mechanism of Plastic Shrinkage Cracking in Portland Cement and Portland Cement-Silica Fume Paste and Mortar, *Cement and Concrete Research*, **20**:103–119.

[3] Bissonnette, B., Pierre, P. and Pigeon, M. 1999. Influence of key parameters on drying shrinkage of cementitious materials *Cement and Concrete Research*, **29**:1655–1662.

[4] Wang, W. 2013. *Plastic shrinkage cracking of cementitious slabs*, Master report, ENPC.

[5] Radocea, A. 1992. *A study on the mechanism of plastic shrinkage of cement-based materials*, PhD thesis, Chalmers University of Technology.

[6] Horpibulsuk, S., Liu, M.D., Liyanapathirana, D.S. and Suebsuk, J. 2010. Behaviour of cemented clay simulated via

the theoretical framework of the Structured Cam Clay model. *Computers and Geotechnics*, **37**:1–9.

[7] Slowik, V., Schmidt, M. and Fritzsch, R. 2008. Capillary pressure in fresh cement-based materials and identification of the air entry value. *Cement and Concrete Composites*, **30**:557–565.

[8] Stakman, W.P. 1966. Determination of pore size by the air bubbling pressure method, *Proceedings Unesco Symp. on water in the unsaturated zone*; pp.366–372